




Heat transfer and pressure drop characteristics of a plate heat exchanger using water based Al_2O_3 nanofluid for 30° and 60° chevron angles

M. M. Elias¹ · R. Saidur^{2,3} · R. Ben-Mansour⁴ · A. Hepbasli⁵ · N. A. Rahim⁶ · K. Jesbains² 

Received: 7 December 2017 / Accepted: 28 March 2018
© Springer-Verlag GmbH Germany, part of Springer Nature 2018

Abstract

Nanofluid is a new class of engineering fluid that has good heat transfer characteristics which is essential to increase the heat transfer performance in various engineering applications such as heat exchangers and cooling of electronics. In this study, experiments were conducted to compare the heat transfer performance and pressure drop characteristics in a plate heat exchanger (PHE) for 30° and 60° chevron angles using water based Al_2O_3 nanofluid at the concentrations from 0 to 0.5 vol.% for different Reynolds numbers. The thermo-physical properties has been determined and presented in this paper. At 0.5 vol% concentration, the maximum heat transfer coefficient, the overall heat transfer coefficient and the heat transfer rate for 60° chevron angle have attained a higher percentage of 15.14%, 7.8% and 15.4%, respectively in comparison with the base fluid. Consequently, when the volume concentration or Reynolds number increases, the heat transfer coefficient and the overall heat transfer coefficient as well as the heat transfer rate of the PHE (Plate Heat Exchangers) increases respectively. Similarly, the pressure drop increases with the volume concentration. 60° chevron angle showed better performance in comparison with 30° chevron angle.

Nomenclature

C Heat capacity rate kJ/K.s.
 c_p Specific heat, kJ/kg.K.
 D Diameter of the port, m.
 G Mass velocity, kg/s.
 h Heat transfer coefficient, $\text{W/m}^2\text{K}$.

k Plate thermal conductivity, W/m K .
 L Port to port length, m.
 \dot{m} Mass flow rate, kg/s.
 N Number of channel.
 NTU Number of heat transfer units.
 Q Heat transfer rate.
 q Actual heat transfer rate.
 T Temperature, K.
 t Thickness of the plate, m.
 U Overall heat transfer coefficient, $\text{W/m}^2\text{ K}$.
 w Effective width of plate, m.
 ΔP Pressure drop, Pa.

✉ K. Jesbains
jesbainss@sunway.edu.my; jesbains5@gmail.com

- ¹ Department of Mechanical Engineering, University of Malaya, 50603 Kuala Lumpur, Malaysia
- ² Research Centre for Nanomaterials and Energy Technology (RCNMET), School of Science and Technology, Sunway University, No. 5, Jalan Universiti, Bandar Sunway, 47500 Petaling Jaya, Malaysia
- ³ Department of Engineering, Lancaster University, Lancaster LA1 4YW, UK
- ⁴ Center of Research Excellence in Renewable Energy (CoRE-RE), Research Institute, King Fahd University of Petroleum & Minerals (KFUPM), Dhahran 31261, Saudi Arabia
- ⁵ Department of Energy Systems Engineering, Faculty of Engineering, Yaşar University, 35100 Izmir, Turkey
- ⁶ UM Power Energy Dedicated Advanced Centre (UMPEDAC), Wisma R & D, University of Malaya, 50603 Kuala Lumpur, Malaysia

Greek symbols

ε Heat exchanger effectiveness.
 ρ Density, kg/m^3 .
 \emptyset Volume fraction.

Subscripts

b Base fluid.
 c Cold.
 eff Effective.
 h Hot.
 nf Nanofluid.
 o Outlet.
 p Nanoparticle.

Dimensionless numbers

Nu Nusselt number.

Pr Prandtl number.

Re Reynolds number.

1 Introduction

The rapid improvements in the past five decades in engineering technology related to fossil and nuclear energy, electric power generation and electronic chips cooling have resulted in acceleration in various subjects associated with heat transfer. Among such subjects is how the numerous engineering systems can cope with problems related to heat transfer improvement in corrugated plate heat exchangers (PHEs). Usually PHEs are broadly used in several engineering applications for their compactness, high thermal efficiency and suitability in variable load as well as ease and flexibility of sanitation. A PHE has attractive features consisting higher surface area due to corrugated channel and mixes the flow field well resulting in an increase in heat transfer. Likewise, PHEs have the flexibility for increasing or decreasing the thermal size (i.e., number of plates) according to heat load requirements. Furthermore, it can be easily disassembled for cleaning, which is important for some cases with strict hygienic constraints, such as pharmaceutical and food processing industries. The PHE performance during the flow degradation is one of the significant subjects that have been incorporated recently [1]. The heat transfer is required to meet the rising demand for higher energy density. This can be accomplished by using fluids with better thermos-physical properties. Nanofluids are relatively fluids with nanometre sized solid particles suspended in a base fluid like water, oil or ethylene glycol. Nanofluids were first invented by Choi [2]. The enhancement of heat transfer using nanofluids is possibly affected by different mechanisms, such as Brownian motion, dispersion of the suspended particles, thermophoresis, diffuseo-phoresis, forming a common boundary at the liquid/solid and ballistic phonon transport [3]. Consequently, the size of the equipment reduction might lead to reduction in expenses and enhancement of the efficiency of heat transfer systems [3].

Extensive research has been carried out previously on the heat transfer characteristics of PHEs experimentally with different chevron angles, herringbone types, etc. [4–7]. However, most of the research has been done on PHEs using conventional fluids, such as water, ethylene glycol as a heat transfer fluid. Unfortunately, conventional fluids have low heat transfer performance. Thus in order to get the required heat transfer performance, enhancement of thermal capability of working fluid is essential. In addition, high compactness and effectiveness of heat transfer systems is also important. Pantzali et al. [8] experimentally studied the efficacy of water based CuO nanofluid with 4 vol.% of nanoparticles as coolants in a

commercial PHE. They have reported that the nature of coolant flow inside the heat exchanger equipment plays a significant role in the effectiveness of nanofluid. On the other hand, Kwon et al. [9] analysed the heat transfer performance and pressure drop of Al_2O_3 and ZnO nanofluids in a PHE. Their investigation concluded that the performance of the PHE at a given flow rate did not increase much when using these nanofluids. Eastman et al. [10] found that the effective thermal conductivity for EG (ethylene glycol) based CuO nanofluid with 0.3% volume concentration is about 40% higher in comparison with base fluid. This indicates that there is room for improvement on heat transfer for commercial purposes. Vajjha and Das [11] used aluminium oxide nanofluids in their study and found that the thermal conductivity increases as the square of the temperature. For example, at 6% particle volume concentration, a raise of 21% thermal conductivity was achieved with the increase in temperature from 298 K to 363 K. Yu et al. [12] studied EG based water nanofluid and concluded that the thermal conductivity mainly depends on the temperature of the fluid because of the higher degree of Brownian motion. Another study was carried out by Godson et al. [13] for the effect of particle material and it was found that the enhancement of thermal conductivity was superior for metal particles nanofluid than metal oxide nanofluids. For instance, at 5% volume concentration, the metal oxide nanofluid had thermal conductivity up to 30%. However, for a volume concentration less than 1.5% of the metal particle nanofluid, improvement in thermal conductivity up to 40% was reported. Lee et al. [14] investigated oxide nanoparticle, such as Al_2O_3 -water, Al_2O_3 -EG, CuO-water and CuO-EG. The thermal conductivity of the nanofluids was measured by a transient hot wire method and it was found that the EG based nanofluid indicated a higher thermal conductivity than the water based nanofluid. Analytical investigation showed that the heat transfer enhancement was found for various heat exchangers using nanofluids with the minimum penalty of pressure drop [13, 15, 16, 17].

The experimental results of the heat transfer and the pressure drop for PHE has very limited literature on it because most of the research has been done through tubes with constant heat flux or temperature. Tiwari et al. [18] experimentally investigated the water based CeO_2 nanofluid in a PHE and found 39% higher heat transfer coefficient compared to water. Most of the research was done by numerically simulating water as a transfer fluid. Huang et al. [19] considered only single corrugation angle (i.e. 65°) in their study. However, our main focus is to investigate the heat transfer and pressure drop characteristics of a corrugated PHE for 30° and 60° chevron angles using water based Al_2O_3 nanofluid. In this study, water based Al_2O_3 nanofluid was chosen due to its reasonable cost and excellent thermos-physical properties. To the best of the authors' knowledge, no experimental work on the heat transfer performance and pressure drop characteristics of a

corrugated PHE for 30° and 60° chevron angles using water based Al₂O₃ nanofluid was found in literature. Therefore, it is expected that this paper can be a new contribution for the aforementioned issues. It was also observed that there are discrepancies exist among different experimental data available in the literature. Therefore, more studies are needed on this to draw a conclusion on the findings with the usage of nanofluids in heat exchangers.

2 Experimental procedure and facility

An experimental set up to investigate the heat transfer and pressure drop characteristics of the corrugated PHE under different nanoparticle volume concentrations is described in this section. The actual plate of the heat exchanger is shown in Fig. 1.

The schematic diagram and the experimental set up of the PHE is illustrated in Fig. 2 and a photograph of the actual system is shown in Fig. 3.

The experiments were carried out using a commercial chevron type (30° and 60°) PHE made from AISI 316 steel. The surface enlargement factor for all the plates were 1.117. Six plates were installed providing five fluid streams (3 cold, 2 hot) in a counter flow arrangement. The experimental set up comprises cold and hot loops. The experimental setup was controlled by A PLC system. A hot water tank with a very high precision heater was used to control the inlet temperature of the hot fluid with an accuracy of ±0.1 °C. The flow rate was adjusted for each run in the PHE to keep the same Reynolds number in both sides. The hot and cold fluids were circulated by a centrifugal 3-stage pump (220/50 Hz, flow range 0.5 to 28 m³/h and maximum pressure 10 bar) through the PHE. Sufficient amount of time was given to achieve steady state conditions before

taking the experimental data. The pressure transducer and thermocouple were placed between the inlet and outlet of the PHE for hot and cold fluids, respectively. The hot fluid flow rate was maintained at 3 L/min. The values for the pressure, the temperature and the flow rate of the PHE were taken from the PLC to determine the convection heat transfer coefficient, the heat transfer rate and the overall heat transfer coefficient. The PHE was arranged in a single pass arrangement and can be changed without disturbing the external piping. The inlet and outlet ports were on opposite sides allowing a counter flow mechanism between two fluid streams. Tables 1 and 2 shows the instruments used for the experimental set up and some geometrical characteristics of the chevron plates, respectively.

2.1 Preparation of nanofluid

In this experiment, the Al₂O₃ nanoparticles were suspended with a base fluid to form the water based Al₂O₃ nanofluid. The average size of the aluminium oxide (Al₂O₃) spherical nanoparticles used in the experiments was 30 nm. The nanofluids were prepared by a two-step method without adding any surfactant. Nanoparticles were added into the base fluid and then sonicated by an ultrasonic machine for 60 min to prepare the nanofluid. Three volume fractions of the nanofluid, ranging from 0.1% to 0.5% of nanoparticles were prepared during the experimental investigation. In order to obtain a good quality of data, the nanofluids were freshly prepared before the experiment for each test to prevent any sedimentation. It is known that both the thermos-physical properties and stability of the suspension mainly depend on the volume fraction, shape, size as well as the thermos-physical properties of the nanoparticles and the base fluid [20]. The volume fraction of the nanofluid was calculated using the following Equation:

$$\varphi = \frac{\frac{m_p}{\rho_p}}{\frac{m_p}{\rho_p} + \frac{m_b}{\rho_b}} \quad (1)$$

2.2 Measurement of thermos-physical properties of nanofluid

2.2.1 Thermal conductivity

The thermal conductivity of nanofluid for different concentration were determined using KD2-Pro (made by Decagon, USA) thermal properties analyser with an accuracy of ±0.1. The sample with a container was put into the temperature controlled bath and temperature of the sample was measured by a thermocouple. The thermal conductivity was measured for different temperature ranging from 25 °C to 55 °C with 5 °C interval.

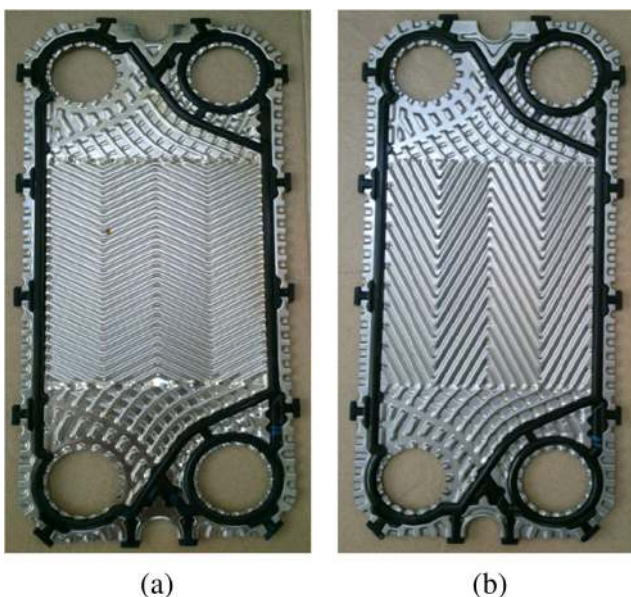
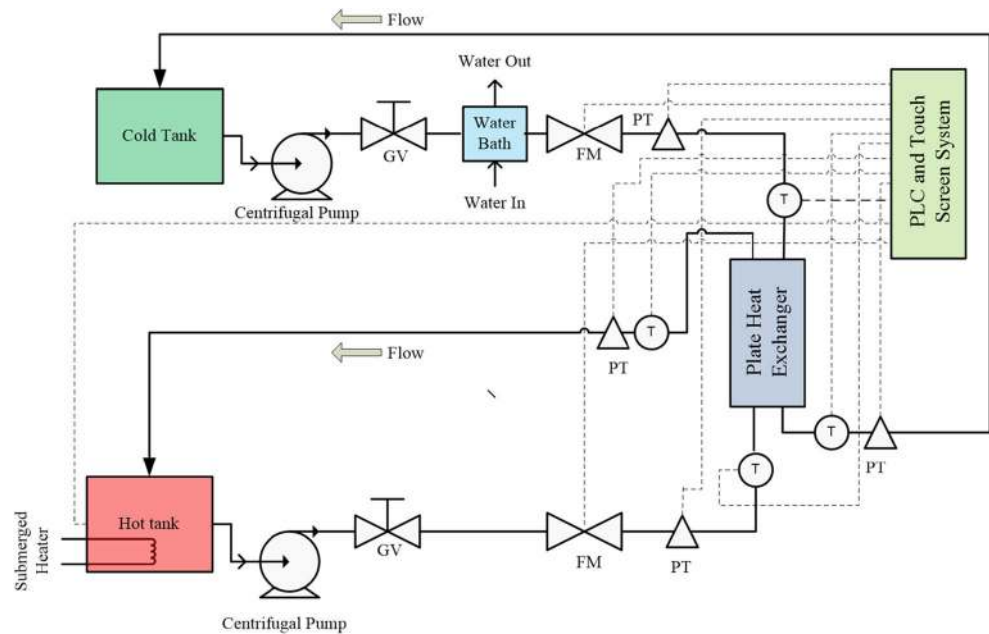


Fig. 1 Heat exchanger plate (a) 60° and (b) 30°

Fig. 2 Schematic diagram of the experimental set up



2.2.2 Density

A portable density meter (KEM-DA 130 N, made by Japan) was used to measure the density of nanofluid. This device can measure the density within the range of 0 to 2000 kg/m³ with the precision of ±0.001 kg/m³. The density was measured within the temperature range of 25 °C to 55 °C.

2.2.3 Viscosity

A Brookfield programmable viscometer (model: LVDV-III ultra) was used to measure the viscosity of the nanofluids within the temperature range of 25 °C to 55 °C with an interval of 5 °C. The viscosity in the range of 1 to 6,000,000 MPa.s was measured using this instrument with the aid of an Ultra low adapter (ULA). In this experiment, the spindle (model ULA-49EAY, spindle code 01) is connected with the viscometer and submerged into the nanofluids.

2.2.4 Specific heat

Specific heat was measured using a differential scanning calorimeter (model: DSC 4000, made by Perkin Elmer, USA) for the different concentrations of nanoparticles. The measurement of specific heat for different temperatures begins from 25 °C, and gradually increased to 55 °C with an interval of 5 °C.

2.3 Thermal performance of the heat exchanger

The heat transfer rate, the convective heat transfer coefficient, and the overall heat transfer coefficient were estimated using the following equations:

The mass flow rate was determined using Eq. (2).

$$\dot{m} = \dot{V} \times \rho \quad (2)$$

Fig. 3 Photograph of the actual experimental set up



Table 1 Instruments used in the experimental set up

No.	Instrument name
1	Plate heat exchanger
2	Pressure transducer
3	Thermocouple
4	Flow meter
5	Water bath
6	Temperature controller
7	Heater
8	Hot tank
9	Cold tank
10	PLC and touch screen

The heat removed by the hot fluid and the heat gained by the cold fluid was determined using Eqs. (3) and (4), respectively.

$$Q_h = \dot{m}_h c_{p,h} (T_{h,i} - T_{h,o}) \quad (3)$$

$$Q_c = \dot{m}_{nf} c_{p,nf} (T_{nf,o} - T_{nf,i}) \quad (4)$$

The fluid properties for the cold and hot fluids were determined using Eqs. (5) and (6), respectively.

$$T_c = \frac{T_{nf,i} + T_{nf,o}}{2} \quad (5)$$

$$T_h = \frac{T_{h,i} + T_{h,o}}{2} \quad (6)$$

The Reynolds number was determined using Eq. (7).

$$Re = \frac{\dot{m} D_e}{N A_c \mu} \quad (7)$$

The Nusselt number was obtained from Eq. (8).

$$Nu_h = 0.348 Re^{0.663} Pr^{0.33} \quad (8)$$

Table 2 Geometrical characteristics of the chevron plates tested in the present study

Parameter	Value
Plate width, L_w (mm)	178.66
Vertical distance between centre of ports, L_v (mm)	394
Port diameter, D_p (mm)	50
Horizontal distance between centre of ports, L_h (mm)	125.98
Corrugation depth or mean channel spacing, b (mm)	2.55 mm
Difference between plate pitch, p	2.90 mm
Plate thickness, t (mm)	0.5 mm
Corrugation pitch, P_c (mm)	14 mm (30°) and 13.5 mm (60°)
Surface enlargement factor, ϕ	1.117
Plate thermal conductivity	0.66 W/m.K
Corrugation angles	30° and 60°

Table 3 Uncertainties associated with the measured values

Parameter	Uncertainties (%)
Hot fluid inlet and outlet temperature, $T_{h,i}$	± 0.2
Cold fluid inlet and outlet temperature, $T_{c,i}$	± 0.2
Ambient temperature, T_a	± 0.15
Hydraulic diameter, D_h	± 2.0
Thermal conductivity measurements of nanofluid, K_{nf}	± 3.0
Density measurements of nanofluid, ρ_{nf}	± 3.5
Viscosity measurements of nanofluid, μ_{nf}	± 4.0
Specific heat measurements of nanofluid, $C_{p,nf}$	± 4.5

$$G_h = \frac{\dot{m}_h}{N b L_w} \quad (9)$$

The channel mass velocity was determined using Eq. (9).

The convective heat transfer coefficient was calculated by Eq. (10).

$$h = \frac{N_u k}{D_e} \quad (10)$$

Where, the hydraulic diameter can be expressed by the Eq. (11).

$$D_e = \frac{2b}{\phi} \quad (11)$$

The overall heat transfer coefficient of the nanofluid was calculated using Eq. (12)

$$U = \frac{1}{\frac{1}{h_c} + \frac{1}{h_h} + \frac{\delta_{plate}}{k_{plate}}} \quad (12)$$

The heat capacity rates for the hot and cold fluids were determined using Eqs. (13) and (14), respectively.

$$C_h = c_{p,h} \dot{m}_h \quad (13)$$

$$C_c = c_{p,nf} \dot{m}_{nf} \quad (14)$$

The effectiveness of the PHE was found from Eq. (15).

$$\varepsilon = \frac{1 - \exp[-NTU(1-C^*)]}{1 - C^* \exp[-NTU(1-C^*)]} \quad (15)$$

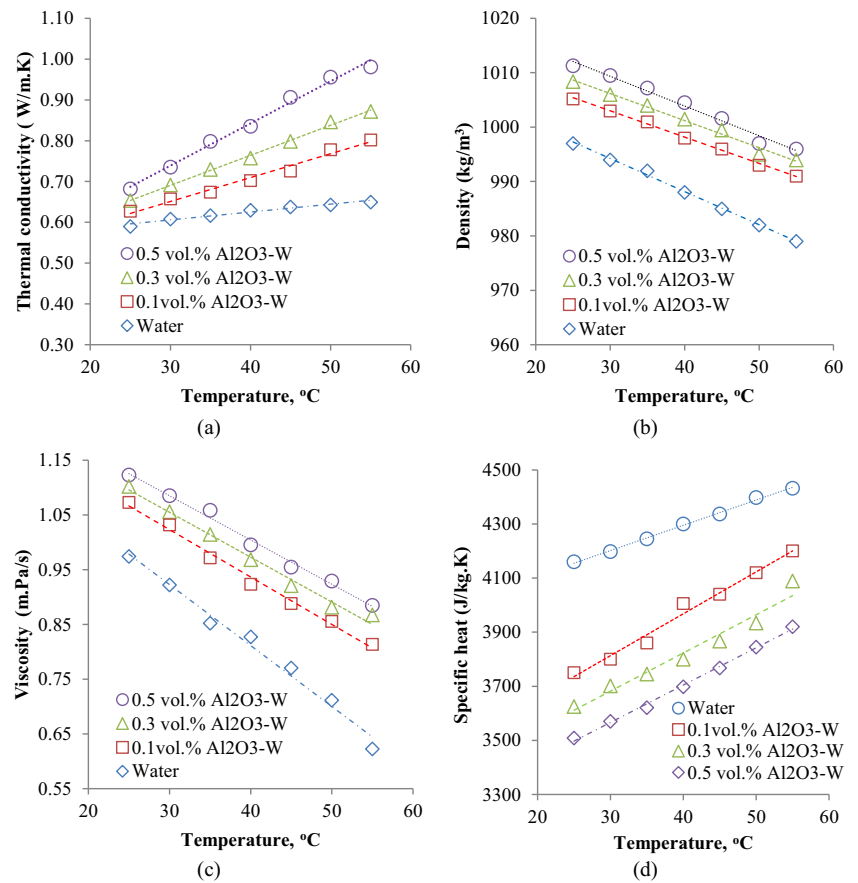
The maximum heat transfer rate was measured using Eq. (16)

$$q_{\max} = C_{\min} (T_{h,i} - T_{c,i}) \quad (16)$$

$$q = \varepsilon q_{\max} \quad (17)$$

The actual heat transfer rate of the PHE was computed from Eq. (17).

Fig. 4 Thermophysical properties of the water based Al_2O_3 nanofluid (a) Thermal conductivity; (b) Density; (c) Viscosity and (d) Specific heat

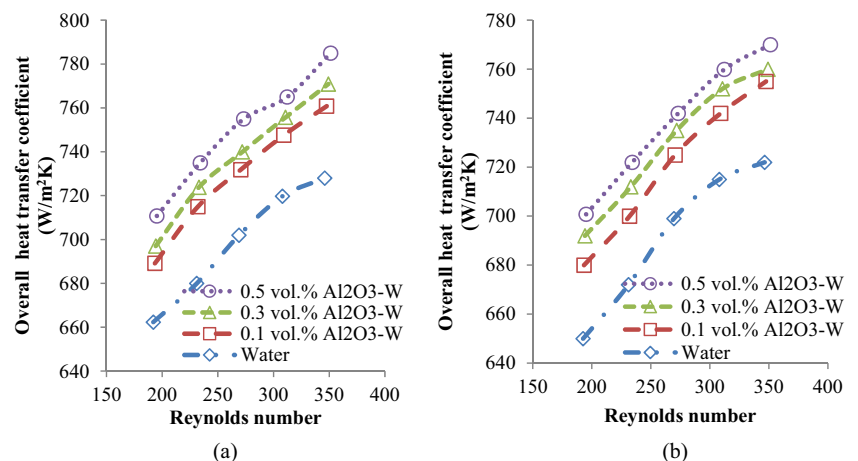


2.4 Experimental uncertainties

$$W_R = \left(\left(\frac{\delta R}{\delta X_1} \omega_1 \right)^2 + \left(\frac{\delta R}{\delta X_2} \omega_2 \right)^2 + \dots + \left(\frac{\delta R}{\delta X_n} \right)^2 \right)^{1/2} \quad (18)$$

The uncertainties associated with the measured values during the experiment are presented in Table 3. The experimental uncertainties were determined using Eq. 18 associated with the related independent variables.

Fig. 5 Variation of overall heat transfer coefficient with the Reynolds number for different coolant volume flow rate (a) 60° , (b) 30° chevron plate

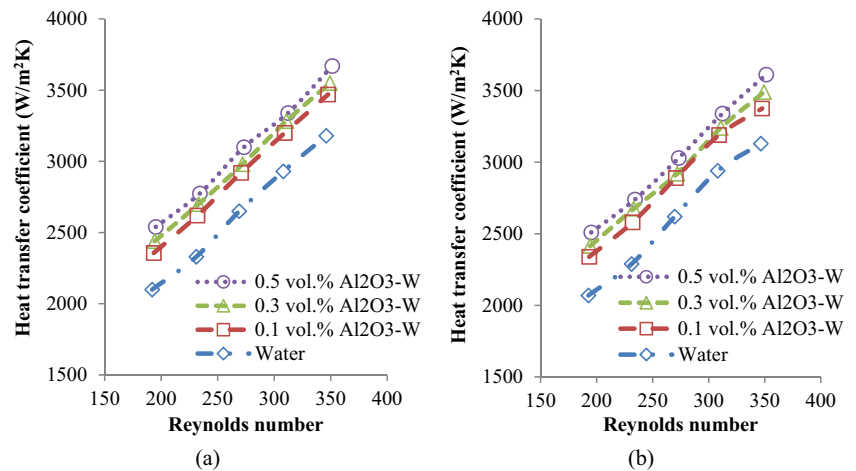


Where, R is the function of independent variables of X_1, X_2, \dots, X_n and $\omega_1, \omega_2, \dots, \omega_n$. W_R represents the uncertainty of dependent variable.

3 Results and discussions

The thermos-physical properties of the nanofluids and the base fluids are essential for the heat transfer analysis of the PHE. For this reason, thermos-physical properties were

Fig. 6 Variation of heat transfer coefficient with the Reynolds number for different coolant volume flow rate (a) 60°, (b) 30° chevron plate



measured experimentally and presented in Figure 4. It has been found from Figure 4(a) that the thermal conductivity of the nanofluid increased with the increase in the volume concentration and the temperature because of the movement of particles during the temperature rise. For instance, the thermal conductivity of the nanofluid at 0.5 vol.% concentration is found 15.64% higher than that of the base fluid at 27 °C whereas it is found 25.25% higher for 55 °C compared to 27 °C. In Fig. 4(b), the density of the base fluid decreased by 1.8% with the increase in the temperature from 25 °C to 55 °C. However, the density increased with volume concentration because of the dispersed nanoparticles in the fluid. It can be seen in Fig. 4(c) that the viscosity of the water based Al₂O₃ nanofluid is decreased by 27.05% when the temperature is increased from 25 °C to 55 °C at 0.5 vol.% concentration. When the temperature of any substance is increased, there will be vigorous movement among the molecules. For the higher movement of the molecules, the resistance to flow of a material is decreased. In Fig. 4(d), the specific heat is increased with increase in temperature. The trend of increase deems constant and almost linear. However, the specific heat is decreased with the increase in the volume concentration,

which is caused due to the lower specific heat of the nanoparticles. In the following subsection, the heat transfer rate, the overall heat transfer coefficient, the heat transfer coefficient and the pressure drop were analysed for the PHE.

3.1 Overall heat transfer coefficient

The overall heat transfer coefficient of the PHE for different chevron angles is portrayed in Fig. 5. In Fig. 5(a), an enhancement of the overall heat transfer coefficient for 0.5 vol.% concentration was found 2%, 3.2% and 7.8% higher than 0.3 vol.%, 0.1 vol.% and water, respectively. In Fig. 5(b), an increment of the overall heat transfer coefficient for 0.5 vol.% concentration was achieved, whereby 1.5%, 2.3% and 6.64% greater than 0.3 vol.%, 0.1 vol.% and water, respectively. Both the cases, 60° chevron angle implements better overall heat transfer coefficient than 30° chevron angle.

3.2 Heat transfer coefficient

The convective heat transfer coefficients in the PHE for 60° and 30° chevron plates is presented in Figure 6. Due

Fig. 7 Heat transfer rates with the Reynolds number for different coolant volume flow rate (a) 60°, (b) 30° chevron plate

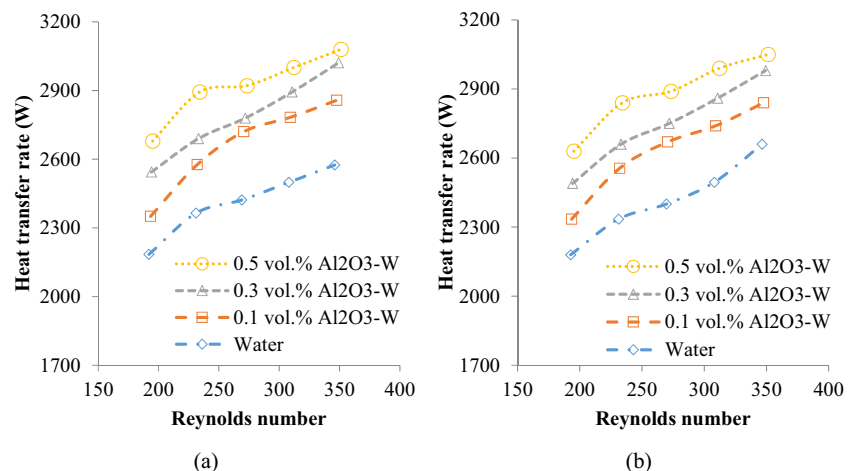
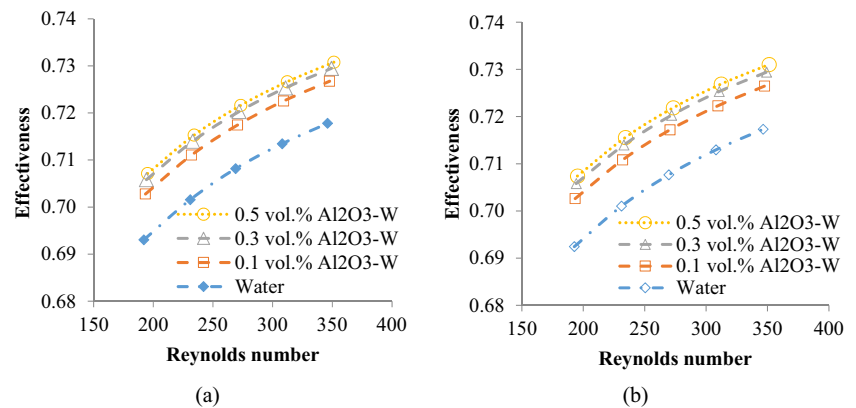


Fig. 8 The effect of nanoparticle concentration on effectiveness as a function of Reynolds number for different chevron angle such as (a) 60°, (b) 30°

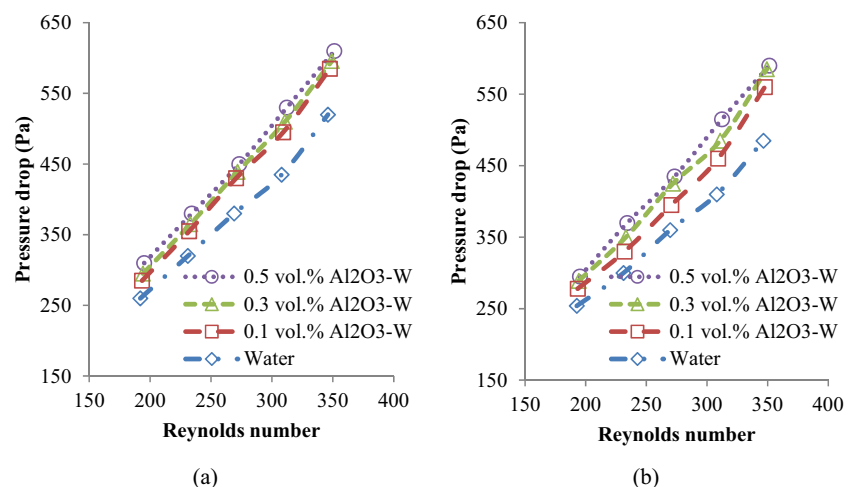


to improved thermos-physical properties of the nanofluid, the heat transfer coefficient was found to be increased compared to the base fluid. By improving the heat transfer coefficient, it is beneficial to the heat exchanger for better thermal performance and energy efficiency. It can be observed from Eq. (10) that the thermal conductivity plays a vital role in enhancing the convective heat transfer coefficient. The heat transfer coefficient is also dependent on the Reynolds number, which is increased with the increase in the nanoparticle vol.% concentration. In Figure 6(a), an enhancement of the heat transfer coefficient for 0.5 vol.% concentration was found to be 3.3%, 5.8% and 15.4% higher than 0.3 vol.%, 0.1 vol.% and water, respectively. In Fig. 6(b), an augmentation of the heat transfer coefficient for 0.5 vol.% concentration was attained 15.3% greater than water. It was observed that PHE with 60° chevron angle performed better than 30° chevron angle for every volume concentration along with the base fluid. The present analysis was done using the heat transfer coefficient with the Reynolds number. The similar trend was found in a study of microchannel heat sink by Chein and Chuang [21].

3.3 Heat transfer rate

Generally, the heat removed from the hot fluid and the heat gained by the cold fluid should be equal. However, practically it is not possible due to the heat loss in the heat transfer process. As shown in Fig. 7 the heat transfer rate is increased with the increase of Reynolds number. It can be determined that the heat transfer rate is higher in nanofluids for different concentrations compared to water for different Reynolds number. In Fig. 7(a), an enhancement of the heat transfer rate for 0.5 vol.% concentration was found 2.5%, 7.8% and 15.14% higher than 0.3 vol.%, 0.1 vol.% and water respectively. In Fig. 7(b), an increase of the heat transfer rate for 0.5 vol.% concentration was achieved 2.3%, 7% and 14.5% higher than 0.3 vol.%, 0.1 vol.% and water respectively. In short, 60° chevron angle performed better than 30° chevron angle for every volume concentration. Various method has been used to compare the nanofluids with base fluids in previous research. Chein & Chuang [21] compared the base fluid with the nanofluid on the velocity basis whereas Pak and Cho [22] compared on the Reynolds number basis. In the present study, the comparison of the heat transfer rate for the water and the

Fig. 9 Pressure drop of plate heat exchanger with the Reynolds number for different coolant volume flow rate (a) 60°, (b) 30° chevron plate



nanofluid were compared by the Reynolds number for different volume flow rates with different volume concentrations.

3.4 Effectiveness

Figure 8 represents the effect of nanoparticle on the effectiveness as a function of Reynolds number. As seen in Fig. 8, the increase of nanoparticle results in enhancement of effectiveness of nanofluid with the Reynolds number. However, the effectiveness of nanofluid is insignificant for the chevron angle of 60° and (b) 30° which can be observed from Fig. 8 as the difference of absolute value of effectiveness for both the chevron angle is so minimal.

3.5 Pressure drop

The major drawback of using nanofluid in the PHE is the increased pressure drop. The pressure drop was measured for different Reynolds number under different coolant volume flow rates as presented in Fig. 9. It is the function of the Reynolds number, the density and the viscosity of the PHE. A higher viscosity is pronounced for higher volume concentration whereas the density increases slightly with the increase of the volume concentration. Chevron angles of 30° and 60° also influences the friction factor. A maximum increase in the pressure drop has been found for higher volume concentration in comparison with the base fluid. In Fig. 9(a), the pressure drop of the PHE for 0.5 vol.% concentration was found 2.3%, 4.2% and 17.3% higher than 0.3 vol.%, 0.1 vol.% and water, respectively. In Fig. 9(b), the pressure drop of the PHE for 0.5 vol.% concentration was attained 1.5%, 5.3% and 19% higher than 0.3 vol.%, 0.1 vol.% and the base fluid water, respectively. Therefore, it is important to carefully select the nanofluid to allow balancing the pressure drop penalty and the heat transfer enhancement.

4 Conclusions

In the present study, we have experimentally investigated thermos-physical properties, the convective heat transfer performance and the pressure drop of water based Al₂O₃ nanofluids in a PHE with chevron angles of 60° and 30°. We have performed experiments for five different Reynolds numbers and three different nanoparticle concentrations. The main conclusions drawn from the results of the present study are listed as follows:

- (a) Thermal conductivity of the nanofluid found to be increased with the increase in the volume concentration and the temperature because of particle movement by Brownian theory during the temperature rise. About 25.25% higher thermal conductivity was found for nanofluids at 55 °C compared to base fluid.
- (b) The maximum overall heat transfer coefficient increase is found to be 7.8% for 0.5% vol.% concentration compared to the base fluid. For 30° chevron angle, the heat transfer coefficient is 6.64% higher than the base fluid.
- (c) Adding the nanoparticle into the base fluid enhances the heat transfer rate of the nanofluid as well as thermal conductivity and convection coefficient and conduction is increased. For 60° chevron plate, a maximum heat transfer rate is found 15.14% higher in comparison with water for 0.5 vol.% concentration whereas it shows 14.5% higher for 30° chevron plate. This means that the plate with 60° chevron angle performs better than 30° chevron angle plate for both nanofluid and water. Moreover, the addition of nanoparticle into the base fluid results in enhancement of effectiveness of nanofluid with the increase of Reynolds number.
- (d) The pressure drop increases with the increasing of volume concentrations. It was found that pressure drop for each run was found higher for the 60° chevron PHE than the 30° chevron PHE.

Acknowledgements The authors would like to acknowledge the “Ministry of Higher Education Malaysia” (MoHE) for the financial support under UM MoHE High Impact Research Grant (HIRG) scheme (Project no: UM.C/HIR/MoHE/ENG/40) to carry out this research. The support of KFUPM to finalize the paper is also acknowledged.

References

1. Abou-El-Maaty T, Abd-El-Hady A (2009) Plate heat exchanger-inertia flywheel performance in loss of flow transient. *Kerntechnik* 74(1–2):35–41
2. Choi S (1995) Enhancing thermal conductivity of fluids with nanoparticles. In: Siginer HPWDA (ed) *Developments applications of non-newtonian flows* (Vol. FED-vol 231/MD-vol). ASME, New York, pp 99–105
3. Wen D, Ding Y (2004) Experimental investigation into convective heat transfer of nanofluids at the entrance region under laminar flow conditions. *Int J Heat Mass Transf* 47(24):5181–5188
4. Ahmed M, Shuaib N, Yusoff M, Al-Falahi A (2011) Numerical investigations of flow and heat transfer enhancement in a corrugated channel using nanofluid. *Int Commun Heat Mass Transfer* 38(10):1368–1375
5. Lotfi R, Rashidi AM, Amrollahi A (2012) Experimental study on the heat transfer enhancement of MWNT-water nanofluid in a shell and tube heat exchanger. *Int Commun Heat Mass Transfer* 39(1): 108–111
6. Mohammed H, Bhaskaran G, Shuaib N, Abu-Mulaweh HI (2011) Influence of nanofluids on parallel flow square microchannel heat exchanger performance. *International Communications in Heat and Mass Transfer* 38(1):1–9
7. Raja M, Arunachalam RM, Suresh S (2012) Experimental studies on heat transfer of alumina/water nanofluid in a shell and tube heat exchanger with wire coil insert. *International Journal of Mechanical and Mater Eng* 7(1):16–23

8. Pantzali M, Kanaris A, Antoniadis K, Mouza A, Paras S (2009) Effect of nanofluids on the performance of a miniature plate heat exchanger with modulated surface. *Int J Heat Fluid Flow* 30(4): 691–699
9. Kwon Y, Kim D, Li C (2011) Heat transfer and pressure drop characteristics of nanofluids in a plate heat exchanger. *J Nanosci Nanotechnol* 11(7):5769–5774
10. Eastman J, Choi S, Li S, Yu W, Thompson L (2001) Anomalously increased effective thermal conductivities of ethylene glycol-based nanofluids containing copper nanoparticles. *Appl Phys Lett* 78(6): 718–720
11. Vajjha RS, Das DK (2009) Experimental determination of thermal conductivity of three nanofluids and development of new correlations. *Int J Heat Mass Transf* 52(21):4675–4682
12. Yu W, Xie H, Chen L, Li Y (2010) Investigation on the thermal transport properties of ethylene glycol-based nanofluids containing copper nanoparticles. *Powder Technol* 197(3):218–221
13. Godson L, Raja B, Mohan Lal D, Wongwises S (2010) Enhancement of heat transfer using nanofluids—an overview. *Renew Sust Energ Rev* 14(2):629–641
14. Lee S, Choi SU, Li S, Eastman J (1999) Measuring thermal conductivity of fluids containing oxide nanoparticles. *J Heat Transf* 121(2):280–289
15. Kakaç S, Pramuanjaroenkij A (2009) Review of convective heat transfer enhancement with nanofluids. *Int J Heat Mass Transf* 52(13):3187–3196
16. Wang X-Q, Mujumdar AS (2007) Heat transfer characteristics of nanofluids: a review. *Int J Therm Sci* 46(1):1–19
17. Huminic G, Huminic A (2012) Application of nanofluids in heat exchangers: a review. *Renew Sust Energ Rev* 16(8):5625–5638
18. Tiwari AK, Ghosh P, Sarkar J (2013) Heat transfer and pressure drop characteristics of CeO₂/water nanofluid in plate heat exchanger. *Appl Therm Eng* 57(1–2):24–32
19. Huang D, Wu Z, Sunden B (2016) Effects of hybrid nanofluid mixture in plate heat exchangers. *Exp Thermal Fluid Sci* 72:190–196
20. Trisaksri V, Wongwises S (2007) Critical review of heat transfer characteristics of nanofluids. *Renew Sust Energ Rev* 11(3):512–523
21. Chein R, Chuang J (2007) Experimental microchannel heat sink performance studies using nanofluids. *Int J Therm Sci* 46(1):57–66
22. Pak BC, Cho YI (1998) Hydrodynamic and heat transfer study of dispersed fluids with submicron metallic oxide particles. *Exp Heat Transfer* 11(2):151–170

Publisher's note

Springer Nature remains neutral with regard to jurisdictional claims in published maps and institutional affiliations.